Internal magnetic focusing in an array of ballistic cavities

Peide D. Ye* and Seigo Tarucha
NTT Basic Research Laboratories, 3-1, Morinosato Wakamiya, Atsugi, Kanagawa, 243-0198, Japan
(Received 26 August 1998; revised manuscript received 15 January 1999)

We study the ballistic motion of electrons in an array of submicron circular cavities, fabricated by electron beam lithography and dry etching techniques. Pronounced magnetoresistance oscillations are observed that can be understood in terms of internal magnetic focusing or commensurability between the electron trajectories and the geometry of the cavities. The depletion distance in the two-dimensional electron gas caused by the dry etching process can be deduced by analysis of the resonance peak positions within a simple magnetic focusing picture. [S0163-1829(99)01216-3]

Ballistic cavities defined in two-dimensional electron gases (2DEG's) provide excellent systems for studying quantum chaotic phenomena. Advancing microstructure technology in semiconductors has revealed a wealth of new physics in these mesoscopic systems. Many previous experimental works have concentrated on the chaotic dynamics of electrons, fractals, electron-electron interactions, quantum interference, and decoherence.[1–4] Reproducible conductance fluctuations (CF's) and weak localization (WL) effects in magnetic fields are analogous to the universal conductance fluctuations and weak localization effects studied in disordered systems. Classical commensurability effects dominate in the magnetoresistance at higher temperatures of an ensemble of cavities, because CF's and WL with quantum mechanical origin are strongly reduced. Although the commensurability between the internal magnetic focusing trajectories and geometry of the cavities has a similar geometric origin as for the experiments of magnetic focusing and commensurability oscillations in an array of antidots,[5,6] few systematic studies have been reported concerning new features in the magnetoresistance at higher temperatures which are related to the classical focusing of trajectories.[7–10] In this paper, we study the ballistic motion of electrons in an array of submicron circular cavities. The dominant conductance fluctuations at lower temperatures are sufficiently reduced by averaging an ensemble of almost identical circular cavities with little realistic difference in the form. Pronounced resonance oscillations are observed in the magnetoresistance measurements which can be understood in the terms of the internal magnetic focusing or the commensurability between the ballistic trajectories and the geometry of the circular cavity. The oscillations survive to a temperature as high as 40 K, demonstrating its classical origin. The peak positions of the magnetoresistance oscillations are consistent with the predicted fields within a simple magnetic focusing model. The depletion distance in the 2DEG caused by the dry etching process is deduced by analysis of the resonance peak positions. Similar experiments on circular cavities with different diameters or electron densities show comparable behavior.

Our samples have been prepared from shallow high-mobility GaAs-$Al_{1-x}Ga_xAs_x$ heterojunctions where the 2DEG is located approximately 40 nm beneath the sample surface. The carrier density n_s and electron mobility μ at 1.6 K are $\sim 3.1\times 10^{11}\,\mathrm{cm}^{-2}$ and $4.2\times 10^5\,\mathrm{cm}^2/\mathrm{V\,s}$, respectively, corresponding to an elastic mean free path, l_e, of 3.9 μm, which is longer than the structure by a factor of 4. 60-μm-wide Hall bars are fabricated by standard photolithography and wet etching techniques. AuGe/Ni pads are alloyed at 450 °C in a reducing atmosphere to make contacts to the 2DEG. Circular cavities with a lithographic diameter d_{lith} of 0.8 and 1 μm are defined by electron beam lithography. After developing the exposed 300-nm-thick polymethylmethacrylate (PMMA) layer of molecular weight 100 000 in methylisobutylketone (MIBK) and isopropyl alcohol (1:2) for 30 sec, the designed patterns are transferred to the semiconductor by electron cyclotron resonance (ECR) dry etching with BCl_3 gas. The etch depth in the devices reported in this paper is 80 nm. After removal of PMMA in acetone, a single circular cavity or an array of circular cavities, like the ones shown in Figs. 1(a) and 1(c), are obtained. Two-point resistance measurements are performed in a ^{4}He and a ^{3}He cryostat with superconducting coils. An ac current with amplitude 10 nA at ~13.5 Hz is applied between two probes and the voltage drop between the same two probes is measured using standard ac lock-in techniques. For all experiments, the external magnetic field B is applied normal (z direction) to the plane of 2DEG. The base temperatures of the pumped ^{4}He and ^{3}He cryostat are 1.6 and 0.3 K, respectively.

The magnetoresistance $R(B)$ of a single circular cavity, and of an array of cavities as a function of perpendicular magnetic fields are shown in Figs. 1(b) and 1(d), respectively. The single cavity shows large resistance fluctuations in Fig. 1(b) at low fields, $|B|\leqslant 0.4\,\mathrm{T}$, which are reproducible as long as the sample is kept at low temperature. The quantum fluctuations are usually largely suppressed above 1 K. The observed CF's with large amplitudes at a temperature of 1.6 K may be related to the very narrow point contacts with a lithographic width of 300 nm. This is consistent with the relatively high zero-field resistance of $\sim h/2e^2$. These kinds of conductance fluctuations are strongly reduced in the trace taken from an array of circular cavities as shown in Fig. 1(d). The cavities are fabricated side by side in one lithographic step. 30 nominally identical but actually slightly different cavities are measured at one time to average out contributions from universal conductance fluctuations. The distance to a neighboring circular cavity is 10 μm, longer than the mean free path of electrons, in order to avoid external mag-

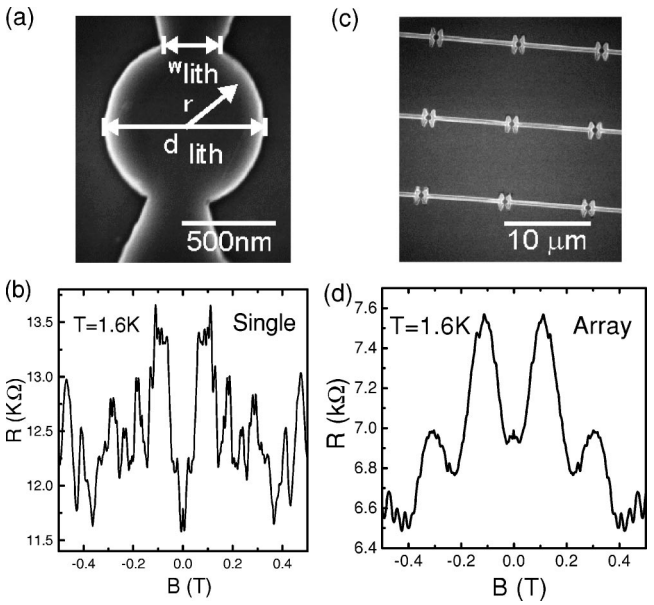

FIG. 1. (a) Electron micrograph of a typical cavity with $d_{lith}=800$ nm, $w_{lith}=300$ nm. (b) Resistance R as a function of perpendicular magnetic field B for a single cavity similar to that shown in (a) but with a diameter of 1 μm. (c) Electron micrograph of an array of circular cavities fabricated side by side with a pitch of 10 μm in one lithographic step using electron beam lithography and dry etching. (d) Resistance R as a function of perpendicular magnetic field B for an array of circular cavities, as shown in (c).

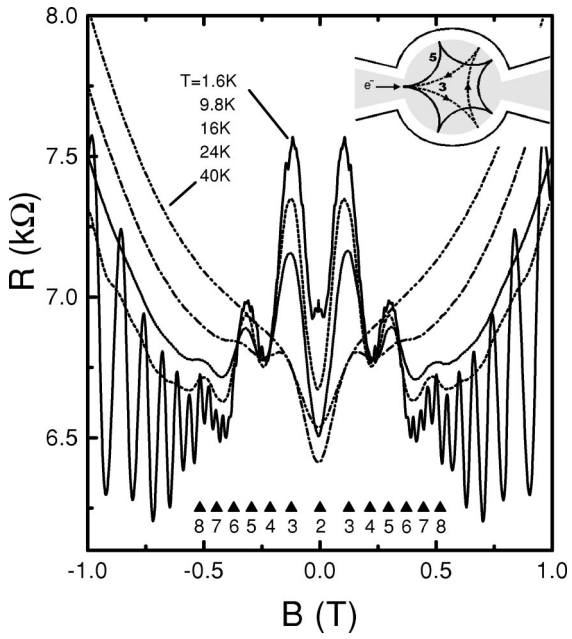

FIG. 2. Temperature dependence of the two-terminal magnetoresistance R for an array of cavities as a function of the external magnetic field B, which is performed in a ^{4}He cryostat from $T=1.6$ to $T=40$ K. The arrows with even numbers mark the minima positions of R as predicted by Eq. (1), whilst those with odd numbers mark the corresponding maxima positions predicted by Eq. (2). The inset indicates the classical electron trajectories related to two of the maxima of the magnetoresistance.

netic focusing between the cavity cells. Small deviations in the shape of the circular cavities from processing lead to different trajectories in each cavity. The different interference phase of the trajectories for each cavity leads to a smearing out of the dominant CF's in a single cavity. The traces in Figs. 1(b) and 1(d) are essentially symmetric, $R(B)\approx R(-B)$, which is the reciprocity relation mandatory for a two-probe measurement of a stable device. Both traces in Figs. 1(b) and 1(d) show narrow resistance peaks at $B=0$ that persist to above 1.6 K. The physical origin of the zero-field peak is presumably coherent backscattering associated with the interference of time-reversed paths, as for weak localization in diffusive electron systems. The line shape of such ballistic WL peaks reveals the dynamic characteristics of the cavities. We return to this point below. As shown in Fig. 1(d), pronounced oscillatory peaks at $B=0.1$ and 0.3 T appear in the trace for the array of cavities. We now concentrate on these magnetoresistance oscillations.

In the ballistic regime, it is illustrative to regard the electron as a ballistic particle moving like a ball. The electron keeps its initial velocity unless it bounces off the confining boundaries or it is affected by the Lorentz force in a magnetic field. Electron magnetic focusing has been performed where the electrons are accelerated by a perpendicular magnetic field and move in cyclotron orbits. After several specula scattering events with the boundary of the circular cavity, electrons can be detected by a second lead. The surface geometrical roughness of the cavity is on a smaller length scale than the electron wavelength. This is a benefit of the low damage to semiconductors by the ECR dry etching. The main feature of the magnetotransport is determined by the specula trajectories of the electrons, which depend on the specula geometry of the cavity. Meanwhile quantum interference effects, such as weak localization and universal conductance fluctuations, also play a role at lower temperatures. One possible way to discern classical resistance oscillations from quantum fluctuations is to increase the temperature. The classical oscillations are far less temperature dependent than the quantum fluctuations. This reflects that the elastic mean free path is less temperature dependent than the phase-breaking length. Figure 2 shows the temperature dependence of two-point magnetoresistance of the device for an array of circular cavities with a diameter of 1 μm. The high symmetry upon reversal of the magnetic field in the magnetoresistance consistent with the reciprocity relation $R(B)\approx R(-B)$ for two-point resistance measurements, indicates that the device is very stable. Shubnikov–de Haas (SdH) oscillations, from which we can estimate the electron density n_s of the device, dominate the magnetoresistance for $B>0.4$ T at a temperature of 1.6 K. Remnants of conductance fluctuations are still observable in the 1.6 K trace for $B<0.4$ T, although an ensemble of 30 circular cavities obviously reduces fluctuations due to different phase of the interference of electrons inside the individual cavities. The sharp ballistic weak localization peak, reflecting the dynamics features of the circular cavities, disappears at higher temperatures. Most of the above quantum interference effects are smeared out and only the classical ballistic effects are left at temperatures higher than 8 K. These classical effects are the central issue of this paper.

The dominant ballistic feature, which survives even for $T\sim 40$ K, is the pronounced maxima in magnetoresistance at $B\approx 0.1$, 0.3 and 0.5 T, which we interpret using the picture

of internal magnetic focusing. At zero magnetic field, electrons are expected to enter the cavity through a point contact and pass straight through the second point contact, i.e., leave the cavity without scattering off the boundary. We estimate four to five channels (not including spin) are occupied by electric modes in the quantum point contacts, by comparing the zero-field resistance of ~ 7 kΩ with the universal resistance h/e^2. If the distance of two quantum point contacts is as large as 1 μm, the resistance of the whole system is the resistance of two quantum point contacts in series.[11] The bulk resistance and the Ohmic contact resistance are negligible compared with h/e^2. At higher temperatures, $T>6$ K, we observe a magnetoresistance minimum at $B=0$ because electrons can leave the cavities immediately without any scattering. In contrast, a sharp peak in the magnetoresistance at $B=0$ appears at lower temperatures because of the ballistic weak localization effect in the cavities. As the magnetic field increases, the electrons are deflected sideways. The electrons are scattered by the boundary and at certain magnetic field a large fraction of the electrons are reflected by the circular cavity boundary back to the entrance point contact. The maxima resistance peaks appear at these particular magnetic fields, B_{max}, when the ballistic electron trajectories are just fully reflected. When ballistic electrons easily leave after colliding a number of times with just one side of the boundary at certain magnetic fields, B_{min}, minima appear in the magnetoresistance. The specific trajectories, shown in the inset of Fig. 2, explain the principle maxima in the magnetoresistance. Because of the simplicity of the circular cavity and the axial symmetry of the two leads, resistance maxima appear at certain fields when electrons just collide with the smooth boundary an even number of times, and are fully reflected to the entrance point contact. This geometric similarity allows us to describe the commensurability effect in a simple way. The magnetoresistance oscillates with minima appearing at B_{min} given by

$$\frac{R_c}{r}=\frac{k_F\hbar}{er|B_{min}|}=\tan(\pi/i), \quad i=2n, \tag{1}$$

and maxima at B_{max} given by

$$\frac{R_c}{r}=\frac{k_F\hbar}{er|B_{max}|}=\tan(\pi/i), \quad i=2n+1. \tag{2}$$

Here, $i=2n$ or $2n+1$ is an integer oscillation index, $n=1,2,\ldots$ is an integer number, R_c is the classical cyclotron radius of electrons at the Fermi energy, $k_F=\sqrt{2\pi n_s}$ is the Fermi wave number, n_s is the carrier density of the 2DEG estimated from SdH oscillations, $\hbar$ is Planck's constant, and r is the effective radius of cavities. The maxima corresponding to $i=3$, 5, and 7 are strikingly observed in the magnetoresistance shown in Fig. 2. The observable order of the maximum resistance is dependent on the mean free path of electrons, specularity at the boundary scattering, and the width of the entrance and exit openings. If l_e is larger than the circumference of the cavity, specular scattering dominates, and as the opening is narrow enough, we should observe much higher order oscillations. Here, the wide lithographic opening of 300 nm prevents the observation of the higher-order maxima. The odd-numbered triangles mark the maxima positions given by Eq. (2) while the even-numbered

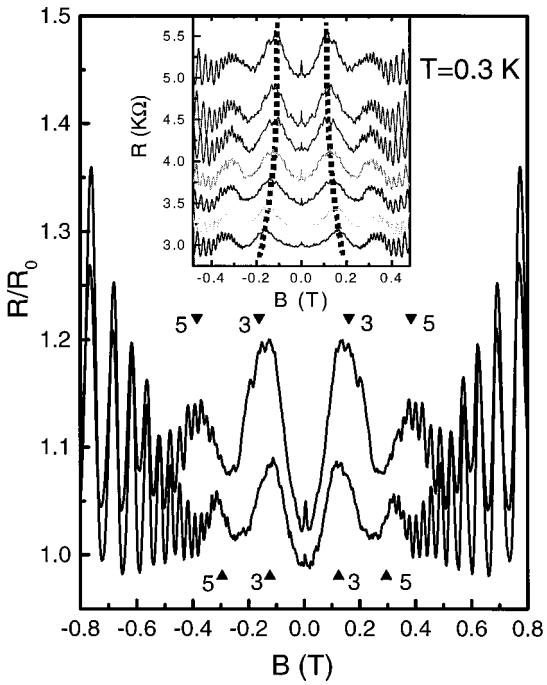

FIG. 3. The two solid lines are the normalized magnetoresistance of an array of circular cavities with diameters of 800 nm and 1 μm. The upper trace is for the case of 800-nm-diameter device and is shifted for clarity. The up-pointing and down-pointing filled triangles mark the corresponding maxima positions predicted by Eq. (2) for different diameters of 1 μm and 800 nm, respectively. The inset shows the electron density n_s dependence of an array of cavities with a diameter of 1 μm. The predicted shift on increasing n_s is indicated by the dashed lines to guide the eye.

triangles identify the minima positions given by Eq. (1), supposing $r=430$ nm. The agreement with the experimental data verifies the validity of this simple picture. We conclude from the rapidly diminishing height of consecutive focusing peaks that there is a probability of diffusive boundary scattering, although the device was fabricated by ECR dry etching with the low damage to semiconductors. The angular dependence of the electron velocity emitted from the quantum point contact has also a contribution. The group velocity of injected electrons $v=\hbar k_x/m$ is roughly proportional to $\cos\phi$, where ϕ is the incident angle of the electrons. The horn-shaped constrictions of quantum point contacts in our devices diminish the diversity of the injected electron velocity.[12] In addition, we are able to deduce that the side depletion distance for an 80-nm-deep ECR dry etch in our devices is ~ 70 nm. This is consistent with the estimate of the effective width of leads (~ 150 nm), which corresponds to approximately four or five open channels.

We fabricated a number of arrays of cavities with different diameters, and in this way we are able to test the model for the commensurability effect of internal magnetic focusing. Figure 3 presents two normalized magnetoresistances for arrays of cavities with lithographic diameters of 800 nm and 1 μm, respectively. The similar magnetic field positions of the minima in the two oscillatory SdH oscillation traces at $B>0.4$ T verifies that the electron density is the same in both cases. The only reason for the resonance peaks in the upper trace to shift to higher magnetic fields is the decrease of the lithographic diameter from 1 μm to 800 nm. The magnetic

field positions of the maxima should be inversely proportional to the effective radius, r, as shown by Eq. (2). The smaller the cavities, the higher the magnetic field positions of the maxima. The down-pointing triangles mark the maxima given by Eq. (2) if $r=330$ nm which corresponds to $d_{lith}=800$ nm, while the up-pointing triangles identify the maxima appropriate for $r=430$ nm, which corresponds to $d_{lith}=1\ \mu$m. The experimental data agrees with the predicted maxima given by Eq. (2). The small features superimposed on the classical resonance oscillations for $B<0.3$ T are the remnants of the conductance fluctuations because of the lower base temperature of 0.3 K. Eq. (2) predicts a similar shift of the maxima to higher field as the electron density n_s has increased. The inset of Fig. 3 shows the n_s dependence of the magnetoresistance for the same array of cavities with a diameter of 1 μm in subsequent illuminations. The zero-field resistance strongly decreases, because more electric channels at the point contacts are opened after illumination. The shift to higher field of the first maxima by increasing n_s is highlighted by the two dashed lines to guide the eye. This qualitatively verifies the validity of Eq. (2). Clearly, Eqs. (1) and (2) predict the main features of such kinds of classical commensurability effects after testing the samples of arrays of cavities with different diameters and electron densities.

Now we address the WL, negative magnetoresistance peak obtained at the lowest magnetic fields. The lineshape of such ballistic WL peaks reveals the dynamic characteristics of the cavities.[2] A striking difference in the line shape of WL peaks is observed with the temperature evolution from $T=0.3$ to 1.5 K. The linearly decreasing triangular line shape only develops *partly* below 0.4 K, showing that phase coherence is essential in producing this shape for the circular cavities. In principle, a nonchaotic system with any coupled leads should exhibit partly chaotic features. The line shape becomes Lorentzian at higher temperatures above 0.6 K, which can readily be fitted by a Lorentzian profile with a half-width magnetic field of 3.5 mT. It corresponds to an area of $0.59\ \mu\text{m}^2$ for the penetration of one flux quantum compared to an estimated area of $0.78\ \mu\text{m}^2$ for the single cavity. The phase breaking rate γ_ϕ is roughly proportional to temperature $\gamma_\phi(s^{-1})=3\times10^{10}\,\text{T}\,(\text{K})$ in a temperature range of 0.6–1.5 K. This is consistent with results from previous experiments.[1,3]

In summary, we have observed pronounced commensurability effects in an array of circular cavities. We are able to correlate specific electron trajectories with maxima and minima in the magnetoresistance with the aid of a very simple internal magnetic focussing model. The validity of this simple model for the commensurability effect is testified by changing the diameter of the cavities, or the electron density of the cavities. The experiment can be applied to deduce the depletion distance in a 2DEG caused by an etching process or gate biasing.

We would like to thank T. Ando and Y. Tokura for fruitful discussions, K. Tsubaki for technical assistance, and D.G. Austing for critical reading of the manuscript. This work was partially supported by a Grant-in-Aid for Scientific Research on the Priority Area ''Spin Controlled Semiconductor Nanostructures'' (No. 09244103) from the Ministry of Education, Science, Sports, and Culture in Japan.

*Present address: National High Magnetic Field Laboratory, Florida State University, Tallahassee, FL 32310.

[1] C. M. Marcus, A. J. Rimberg, R. M. Westervelt, P. F. Hopkins, and A. C. Gossard, Phys. Rev. Lett. **69**, 506 (1992).

[2] A. M. Chang, H. U. Baranger, L. N. Pfeiffer, and K. W. West, Phys. Rev. Lett. **73**, 2111 (1994).

[3] J. P. Bird, K. Ishibashi, D. K. Ferry, Y. Ochiai, Y. Aoyagi, and T. Sugano, Phys. Rev. B **51**, 18 037 (1995).

[4] R. P. Taylor, R. Newbury, A. S. Sachrajda, Y. Feng, P. T. Coleridge, C. Dettmann, Ningjia Zhu, Hong Guo, A. Delage, P. J. Kelly, and Z. Wasilewski, Phys. Rev. Lett. **78**, 1952 (1997).

[5] H. van Houten, C. W. J. Beenakker, J. G. Williamson, M. E. I. Broekaart, P. H. M. van Loosdrecht, B. J. van Wees, J. E. Mooij, C. T. Foxon, and J. J. Harris, Phys. Rev. B **39**, 8556 (1989).

[6] D. Weiss, M. L. Roukes, A. Menschig, P. Grambow, K. von Klitzing, and G. Weimann, Phys. Rev. Lett. **66**, 2790 (1991).

[7] Y. Hirayama, S. Tarucha, T. Saku, and Y. Horikoshi, Phys. Rev. B **44**, 3440 (1991).

[8] H. Linke, L. Christensson, P. Omling, and P. E. Lindelof, Phys. Rev. B **56**, 1440 (1997).

[9] I. V. Zozoulenko, R. Schuster, K. F. Berggren, and K. Ensslin, Phys. Rev. B **55**, R10 209 (1997).

[10] P. Bøggild, A. Kristensen, H. Bruus, S. M. Reimann, and P. E. Lindelof, Phys. Rev. B **57**, 15 408 (1998).

[11] Y. Hirayama and T. Saku, Phys. Rev. B **41**, 2927 (1990).

[12] C. W. J. Beenakker and H. van Houten, in *Solid State Physics*, edited by H. Ehrenreich and D. Turnbull (Academic, San Diego, 1991), Vol. 44.